Experiments on synthetic data

Sylvain Chevillard

November 15, 2013

1 Construction of the magnetization

The goal of these experiments is to construct a realistic example of magnetization, with a relatively small support, and simulate measurements of the magnetic field produced by this magnetization. These simulated measurements can then be used to test techniques designed to recover the net moment and/or the support and the magnetization itself. The advantage being that the quality of the recovered data is easily determined, since we perfectly know the true magnetization.

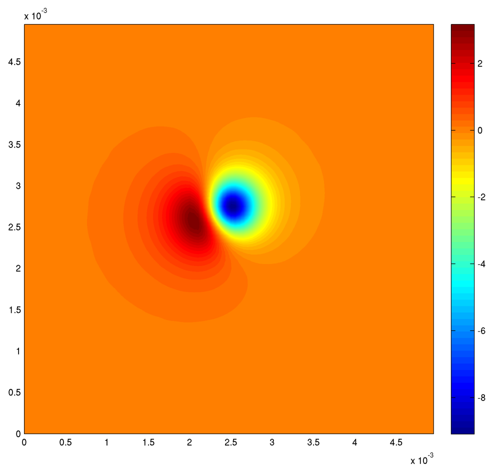

Figure 1: B_z as provided by file `Lonar-6_IRM200mT.mat`. Height between magnetization plane and measurements plane: 2.7 e−4. Sampling step on the measurements plane: 5 e−5. Measurements rectangle is 100×100.

In order to produce a realistic magnetization, we try to do something that roughly looks like the Lunar Spherule example (cf. Figure 1). In order to simulate a continuous magnetization, we consider a grid with sampling step 10 times smaller than the measurement grid on which we put dipoles. The support of the magnetization is included in a 83×105 rectangle. Its shape is the dot of the 'i' of the Inria logo. A main direction is chosen. The dipoles roughly all point in that direction, but they also have a small but non-trivial component in the orthogonal space of that direction. This orthogonal component is not the same for all dipoles and varies smoothly. The three components of the magnetization are represented in Figure 2. The main direction and the amplitude of the dipoles forming the magnetization are chosen so as to look like the lunar spherule example. The normal component B_z of the field produced by the magnetization is shown on Figure 3.

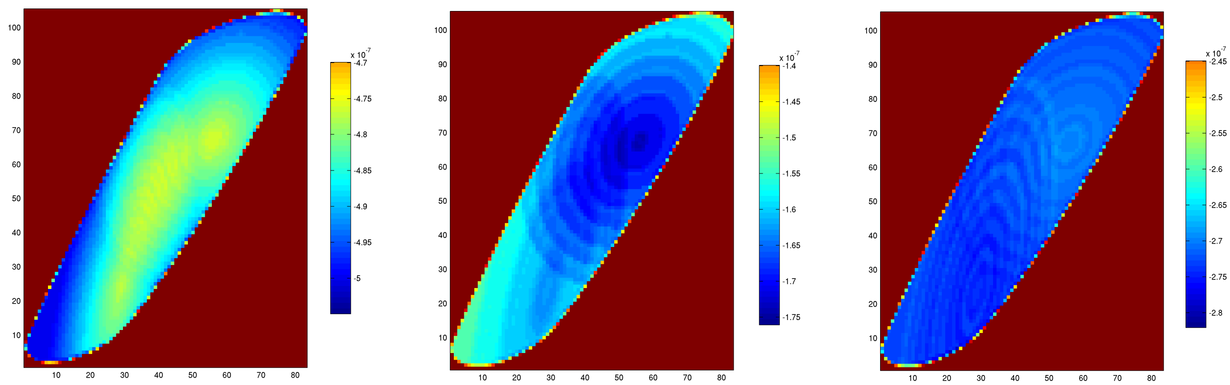

(a) m_1 (b) m_2 (c) m_3

Figure 2: The three components of the true magnetization. Dark red means 0. The magnetization is formed of dipoles with all roughly the same moment $-(5,\, 1.5,\, 2.75) \cdot 10^{-7}$.

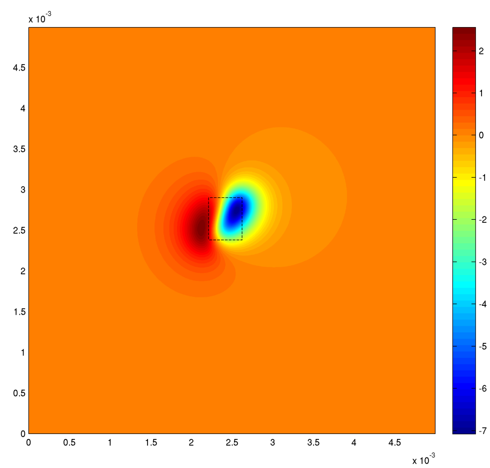

Figure 3: B_z produced by our synthetic magnetization. The rectangle drawn with a dotted line shows the position of the rectangle supporting the magnetization, below the measurement plane.

2 Simulating measurements

In order to simulate measurements of the field, we keep only value of B_z on a 100×100 grid (covering the same square as in Figure 3. Moreover, we add noise at all points (i, j) of the grid by replacing the true value $B_z(i, j)$ by $B_z(i, j)\,(1 + \epsilon(i, j)) + \delta(i, j)$, where ϵ is a random variable following a normal distribution with mean 0 and standard deviation 0.01, and where δ is a random variable following a normal distribution with mean 0 and standard deviation 0.0005. It is not easy for me to tell if this is realistic or not. In Figure 4, one can compare the measures of B_z in the lunar spherule example and in the synthetic example. In order to see how the measures behave when they are close to 0, scales have been saturated.

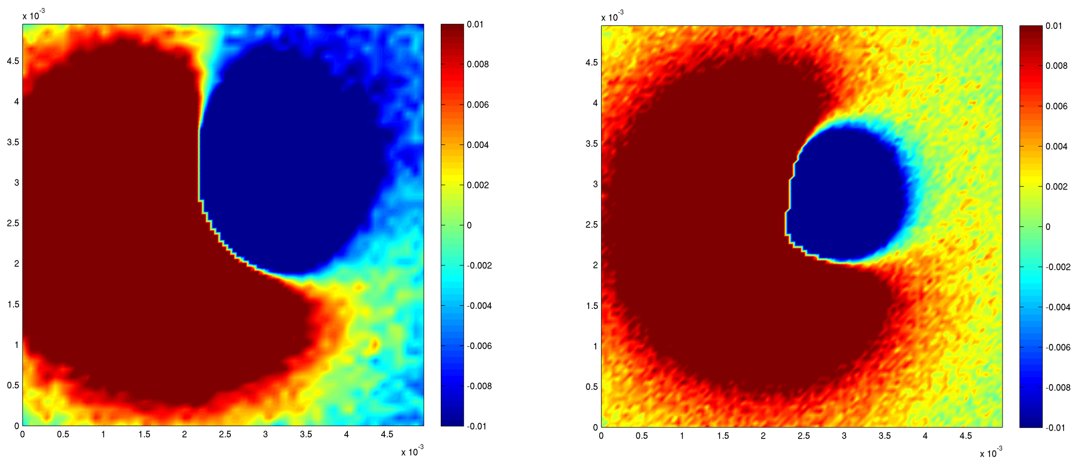

(a) Lunar spherule

(b) Synthetic example

Figure 4: Comparison of measurements of B_z with saturated scale, on the lunar spherule example and on our synthetic example. Everything smaller than -0.01 is colored in dark blue. Everything above 0.01 is colored in dark red.

3 Trying to recover the magnetization

At first, we assume that we do not know anything about the support of the magnetization: all we have is a thin plate (on which the magnetization is indeed quasi-punctual, but we do not know it) and we measured the normal component of the magnetic field above it, on the whole surface of the thin plate. And this gave us the noisy measures of Figure 4b.

We consider a magnetization grid covering the whole rectangle, but with sampling step three times bigger than the sampling step of the measurement grid. Our candidate magnetization grid is hence a rectangle of 34×34 points. We will look for a combination of dipoles positioned at the nodes of this grid, and which would explain the measures the best as possible.

For this purpose, we consider the discrete linear operator A that maps the dipoles ($3 \times 34 \times 34$ variables) on the measurements (100×100 values). We solve the least squares problem of finding $\min_x \|Ax - b\|_2$ where b denotes the vector of measurements of B_z. More precisely, we construct the matrix $M = A^\star A$ (square matrix with $3 \times 34 \times 34$ rows and columns). This computation takes about 7 minutes on an Intel(R) Xeon(R) W3520 CPU at 2.67 GHz with 4 GB of RAM.

3.1 Singular value decomposition

Then we perform a singular value decomposition $V' S V^\star = M$ of M. This computation takes about half a minute on the same computer. Since M is a symmetric positive matrix, it is diagonalizable with non-negative eigenvalues and therefore, any eigenvector of M^2 is also an eigenvector of M. Besides, $M^\star M = M^2 = VS^2V^\star$ which shows that any column of V is an eigenvector of M^2. In conclusion, any column of V is also an eigenvector of $M = V'SV^\star$, and so, the k-th column of V' equals the k-th column of V for any k such that $s_k \neq 0$.

This leads to two remarks: first, it gives a way of testing the numerical quality of the computed decomposition: one may compare the columns of V and V' coefficient-wise, to check that they agree, up to small roundoff errors. The fact that they agree does not mean much in itself, but if they disagree, we can be sure that something is going wrong. Second, this recall us that, in the case of a symmetric matrix, computing a SVD or diagonalizing the matrix is essentially the same. The decomposition may hence be obtained through the `eig` command of Matlab. It turns out to that it is slightly faster (25 seconds are needed to perform the diagonalization) but seems less accurate. The matrix V obtained by diagonalization might be different if some eigenspaces have dimension greater than 1.

Now, if we consider a singular value decomposition $T\Sigma W^\star = A$ of A, we see that $W\Sigma^2W^\star$ is a singular value decomposition of $A^\star A$, and therefore, the columns of W form an eigenvector basis of $A^\star A$. Thus, $\Sigma = \sqrt{S}$ and it easy to see that, forming linear combinations of the columns of T corresponding to columns of W lying in a common eigenspace, there exists an orthogonal matrix U such that $U\Sigma V^\star = A$. Notice that it is not reasonable to compute the whole matrix U because it is way too large to be stored in the RAM.

In the following, we will denote by v_k (respectively u_k) the k-th column of V (respectively U). Accordingly, we will denote by σ_k the k-th singular value of A. Theoretically speaking, the vector x minimizing $\|Ax - b\|$ satisfies $A^\star Ax = A^\star b$, i.e. $x = VS^{-1}V^\star A^\star b$. We denote by $(x_1, \ldots, x_N)^T$ the column vector $S^{-1}V^\star A^\star b$, i.e. the coefficients of x in the basis of the singular vectors (v_k). Finally, we denote by $x^{(k)}$ the orthogonal projection of x onto $\mathrm{Span}(v_1, \ldots, v_k)$, i.e. $x^{(k)} = \sum_{i=1}^{k} x_i\, v_i$.

3.2 Characteristics of the solution

We remark that the matrices U, Σ and V only depend on the map A, and not on the actual measurements b. They are in fact defined by the geometry of the magnetization and measurement grids. In our case, both grids have the same physical dimension but the sampling step of the magnetization grid is 3 times larger than the sampling step of the measurement grid. We observe in Figure 5 that the singular values of $A^\star A$ are rapidly decreasing. Those that are really important are the singular values of A, but still, they decrease from roughly 2^{17} to 2^4.

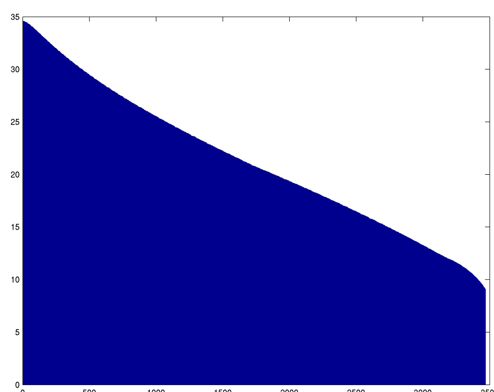

Figure 5: Binary logarithm of the k-th singular value of $M = A^\star A$ in function of k

The singular vectors v_k can be interpreted as magnetization with total energy 1, but leading to measurements of total energy σ_k. It is interesting to look how the amplitude of the net moment of the magnetization v_k varies with k. This is shown in Figure 6. As can be seen, there is no clear relation between the amplitude of the net moment of v_k and k. In particular, there are magnetizations (those corresponding to large values of k) which are almost silent, but which have a non trivial net moment. This is not a good news, since it probably means that the measurements can be very well approximated by magnetizations with almost arbitrary moments.

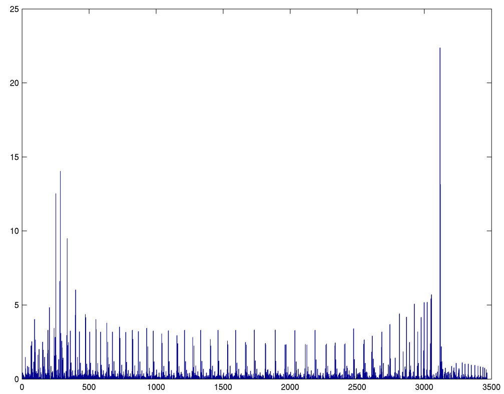

Figure 6: Amplitude of the net moment of the k-th singular vector v_k in function of k

This intuition is confirmed by facts. In Figure 7, the norm of $Ax^{(k)} - b$ is represented in function of k. As can be seen, it is almost constant from roughly $k = 1500$ to the end. More precisely, $\|Ax^{(3468)} - b\| \simeq 0.8168$ whereas $\|Ax^{(1500)} - b\| \simeq 0.9282$. Remark that $x^{(3468)}$ is the solution of least squares problem, so it is not possible to obtain a smaller norm than 0.8168. These residual norms should be compared to the norm $\|b\|$ of the measurements, i.e. roughly 47.70 in this case.

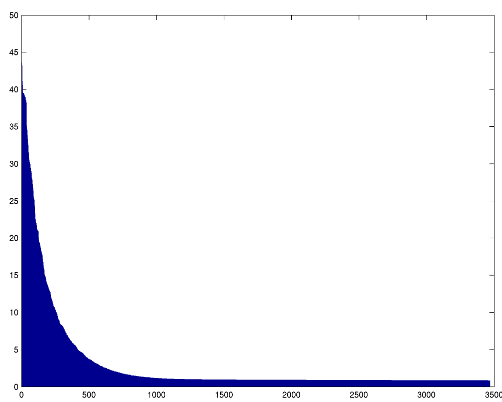

Figure 7: $\|Ax^{(k)} - b\|_2$ in function of k

It follows from this observation that any $x^{(k)}$ with $k \geq 1500$ explains the data practically as well as $x^{(3468)}$ itself, and it is not possible to decide whether one is more realistic than another, without further information. Figures 8 and 9 show the amplitude and direction of these x^k (in blue) together with the amplitude and direction of the true net moment of our synthetic magnetization (in red). We see that none of the $x^{(k)}$ leads to correct values, which suggests that **it is not possible to recover the net moment** of the magnetization that produces the given data without further information.

3.3 Support shrinking

The magnetization x that minimizes $\|Ax - b\|$ spreads on the whole magnetization grid. However, since the true magnetization has a very small support, the recovered magnetization remains fairly localized, in the

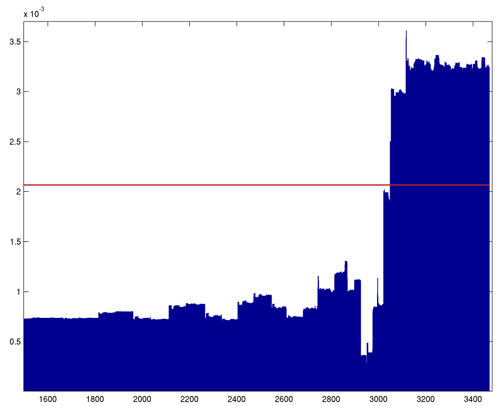

Figure 8: Amplitude of the net moment of $x^{(k)}$ in function of k, for k varying from 1500 to $3 \times 34 \times 34$. The red line corresponds to the amplitude of the net moment of the true magnetization.

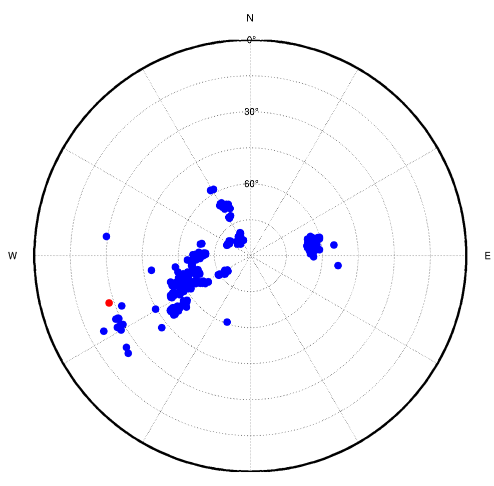

Figure 9: Direction of the net moment of $x^{(k)}$ in function of k, for k varying from 1500 to $3 \times 34 \times 34$. The red dot corresponds to the direction of the net moment of the true magnetization.

sense that, on most of the points of the grid, it takes values that are fairly small. Figure 10 shows the points of the grid where the recovered magnetization has a significant amplitude (light color), in contrast with the points where it has a small amplitude (in dark color). More precisely, for each of the three components of the recovered magnetization, we consider the maximal absolute value taken on the grid and select those points of the grid for which the corresponding component is at least 10% of the max. The points drawn with the light color correspond to the points for which at least one of the three components of the magnetization has been selected by that process. The whole grid contains $34 \times 34 = 1156$ points, whereas there are only 101 selected points.

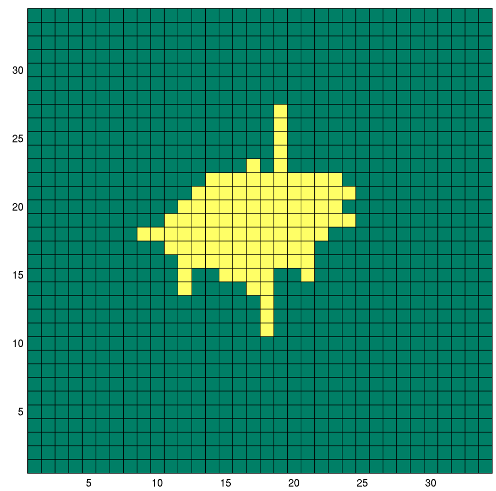

Figure 10: New support: the points of the grid with the dark color are discarded for next step.

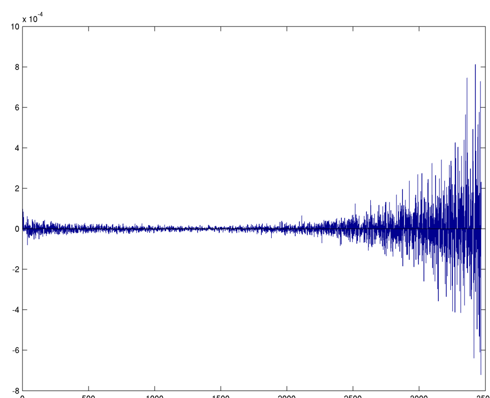

Figure 11: Coefficients x_k of the vector x minimizing $\|Ax - b\|_2$ expressed in the basis of the singular vectors (v_k).

3.4 Second step, with reduced support

We consider now the discrete linear operator A_2 that maps dipoles disposed on the new support (3×101 variables) to the measurements (still 100×100 values). We proceed as before, but using A_2 instead of A.

The shape of the singular values of A_2 is strongly similar to the corresponding one for A, as can be seen on Figure 12 (to be compared with Figure 5).

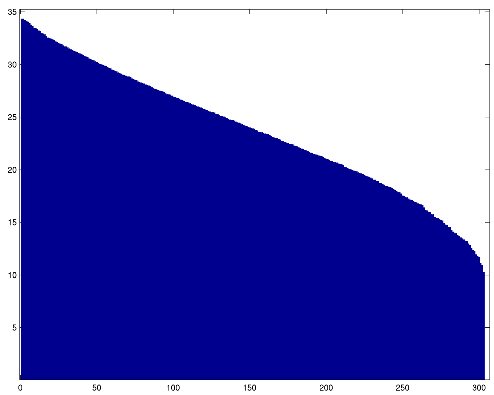

Figure 12: Binary logarithm of the k-th singular value of $M = A_2^\star A_2$ in function of k

On the contrary, the amplitude of the net moment of the successive singular vectors has a much nicer form for A_2: the amplitude is roughly decreasing with the index of the singular vector, which means that the contribution of the last singular vectors to the overall net moment should be negligible (see Figure 13).

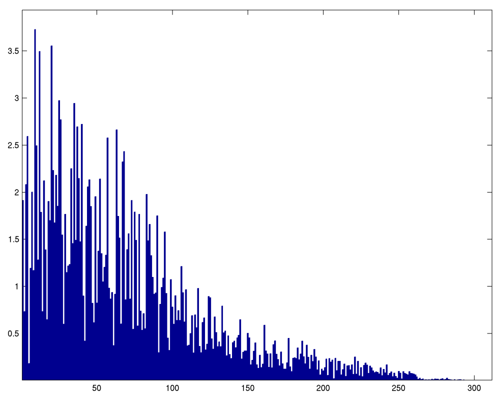

Figure 13: Amplitude of the net moment of the k-th singular vector v_k in function of k

Again, we observe that $\|Ax^{(k)} - b\|$ is almost constant once k is large enough (Figure 14). More precisely, $\|Ax^{(303)} - b\| = 0.8393$ while $\|Ax^{(150)} - b\| = 1.018$. Of course, even $\|Ax^{(303)} - b\|$ is larger than what we had during the first try. This is is because the magnetization grid that we consider for this second try is a subset of the magnetization grid used for the first try. However, one can notice that the residual is not much bigger now than before, which means that we did not loose something significant by reducing the support: we now explain the data almost as well, but with much less dipoles.

In contrast with what we observed for the first try, the net moment of $x^{(k)}$ is now fairly constant in the range of k for which $\|A_2x^{(k)} - b\|$ is roughly constant. See Figures 15 and 16. Moreover, it approximates fairly well the net moment of the true magnetization. Namely, the ratio between the amplitude of the net moment of the true magnetization and the amplitude of the net moment of the magnetization $x^{(303)}$ minimizing $\|A_2x - b\|$ is 1.04. There is only a difference of about 2.25 degrees between their directions.

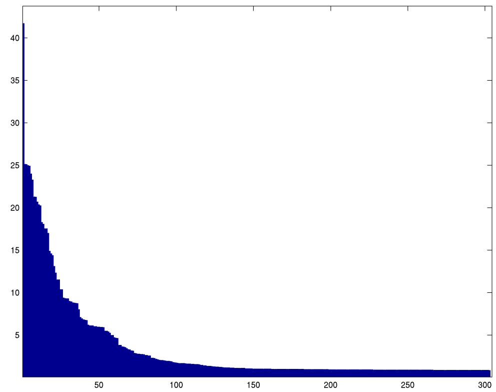

Figure 14: $\|A_2x^{(k)} - b\|_2$ in function of k

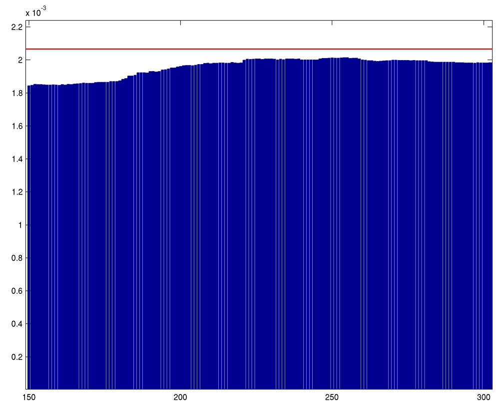

Figure 15: Amplitude of the net moment of $x^{(k)}$ in function of k, for k varying from 150 to 3×101. The red line corresponds to the amplitude of the net moment of the true magnetization.

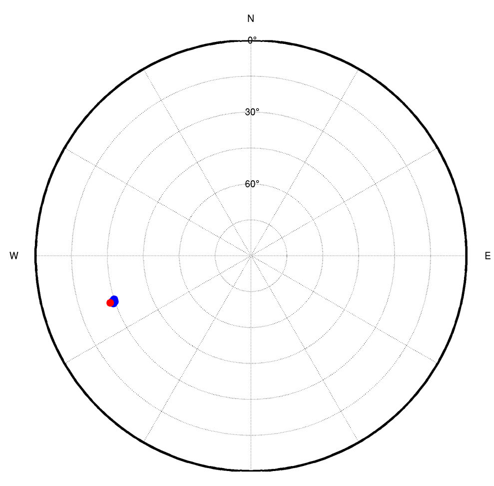

Figure 16: Direction of the net moment of $x^{(k)}$ in function of k, for k varying from 150 to 3×101. The red dot corresponds to the direction of the net moment of the true magnetization.

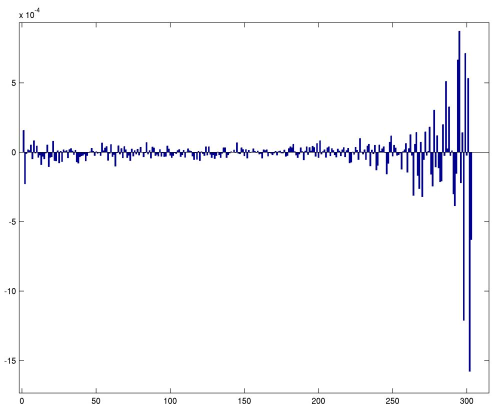

Figure 17: Coefficients x_k of the vector x minimizing $\|A_2x - b\|_2$ expressed in the basis of the singular vectors (v_k).